The Diamond Nano-Balance

Non Peer-reviewed author version

WILLIAMS, Oliver; MORTET, Vincent; DAENEN, Michael & HAENEN, Ken (2009) The Diamond Nano-Balance. In: JOURNAL OF NANOSCIENCE AND NANOTECHNOLOGY, 9(6). p. 3483-3486.

DOI: 10.1166/jnn.2009.NS20
Handle: http://hdl.handle.net/1942/9835

The Diamond Nano-Balance

Oliver A Williams,[a),1,2] Vincent Mortet[1,2], Michael Daenen[1] and Ken Haenen[1,2]

[1]Hasselt University, Institute for Materials Research (IMO), Wetenschapspark 1, B-3590 Diepenbeek, Belgium
and
[2]IMEC, Division IMOMEC, Wetenschapspark 1, B-3590 Diepenbeek, Belgium
(Michaël is not IMEC.)

ABSTRACT

Detecting nano-gram quantities of analyte in the liquid or gas phase is crucial for pathogen detection, antigen/DNA detection, water monitoring, electrochemical analysis, and many other bio-electrochemical applications. The quartz crystal microbalance (QCM) has become a significant sensor for both liquid and gas phase graviometry due to its high sensitivity, robustness, ease of use and simultaneous electrochemistry capabilities. One key factor plaguing the QCM in most sensor applications is the stability of the surface functionalisation. Diamond offers the most stable surface for functionalisation, the widest electrochemical window and the lowest noise floor. Unfortunately the growth of diamond on QCMs is problematic due to the low curie point of quartz, resulting in the loss of the piezoelectric properties of the QCM. In this work the replacement of the quartz with a high temperature stable piezoelectric material is proposed, and a nanocrystalline diamond coated sensor demonstrated.

[a)] Corresponding author: oliverwilliams@mac.com

1. INTRODUCTION

In 1959 the foundations of what is now the Quartz Crystal Microbalance (QCM) were laid down in the derivation of the Sauerbrey equation, which related the shift in resonant frequency of an oscillator with applied mass for a bulk acoustic wave oscillator.[1] Thus micro-graviometry was born and in the nearly 50 years since, the QCM has been implemented in practically every laboratory in the world, be it for simple vacuum deposition monitoring, immunosensing[2], DNA detection[3] or sophisticated macro-molecule visco-elastic characterisation.[4] Following the discovery that QCMs can operate in liquids,[5] further development of the technique lead to simultaneous electrochemistry[6] and visco-elastic measurements. As techniques expand in complexity, so do the amount of variables and parameter space. For the QCM, one of the most complicated areas is the surface and it's associated stability. For many simple applications such as thermal evaporation and magnetron sputtering monitoring this is not crucial, but for monitoring antibody-antigen interactions for example, the long-term stability of the surface functionalisation is critical. For most QCM electrodes this is rather poor, such as gold thiol strategies. Diamond has been shown to exhibit the most stable functionalised surface of all the semiconductors,[7] and this could be a crucial advantage for pathogen detection, immunosensing, toxin monitoring, stripping voltammetry etc. Diamond also exhibits low friction,[8] extreme chemical stability and bio-inertness,[9] tuneable wettability to the nano scale with simple stable surface terminations[10] and the widest electrochemical window / lowest noise floor for electrochemical electrodes.[11] Thus a conductive diamond coating could be particularly interesting for biological and electrochemical QCM applications. Unfortunately the curie point of quartz is below that of conventional

diamond deposition temperatures,[12] rendering the resulting sensor non – piezoelectric. Attempts to grow diamond at lower temperatures have also failed presumably due the loss of the piezoelectric properties at temperatures significantly below the phase transition. Limited success has been achieved by the bonding of freestanding diamond to QCM elements,[13] but this results in highly reduced Q and is not commercially viable due to the thickness required for mechanical stability of the freestanding diamond (>20 μm).

The novel solution we present here is to replace the quartz of the QCM with a high temperature stable piezoelectric such as Langasite[14] or Gallium Orthophosphate.[15] These materials can withstand the high temperatures of the growth environment and have the added advantage of higher piezoelectric coupling coefficients. Table 1 compares and contrasts the relevant properties of these modern piezoelectric materials. It can be seen from this table that the curie temperatures of these materials are significantly higher than the temperature of conventional diamond growth. This table also shows the piezoelectric coupling efficiency can be two to three times higher than that of quartz which can be a considerable advantage in liquid operation or in situations with high damping.

2. EXPERIMENTAL DETAILS

Commercially sourced langasite and gallium orthophosphate crystals were used throughout. For proof of principal, SiO_2 was magnetron sputtered on top of an electrode of a langasite thickness shear mode resonator. This layer was then seeded with a monodisperse diamond nanoparticle aqueous based colloid, known to yield nucleation densities higher than 10^{11} cm^{-2}.[16] Nanocrystalline diamond was then grown by microwave enhanced chemical vapour deposition in an ASTeX 6500 series reactor. The growth conditions were 3% CH_4 diluted by H_2, 700 ºC as monitored by a dual wavelength pyrometer, 3500 W microwave power, process pressure 30 Torr for 10 mins. These conditions are known to produce high quality microcrystalline and nanocrystalline diamond in this reactor.[17] A schematic of the device is shown in figure 1(a). A second prototype was fabricated by utilizing an electrode of tungsten, known for its small carbon diffusion coefficient resulting in thin carbide layers and early diamond nucleation.[18] This layer was also seeded by the aforementioned nanodiamond colloid. Nanocrystalline diamond was carried out under the same conditions except for the addition of 5000 ppm trimethylboron into the gas phase to render the diamond p - type and metallically conductive. Thus the diamond / W / Carbide sandwich acts as one electrode for the thickness shear mode resonator. The other electrode was deposited by magnetron sputtering at a base pressure better than $1x10^{-6}$ Torr. A Schematic of this device is shown in figure 1(b).

Frequency analysis of the resonators was performed using a Hewlett Packard HP4194A network analyser operated in the gain phase mode with a drive voltage of 0.125 V. This

drive voltage is one tenth of that used to resonate typical quartz crystals due to the enhanced coupling factor of langasite and $GaPO_4$.

3. RESULTS AND DISCUSSION

The gain phase properties of the prototype langasite oscillator shown in figure 1(a) are shown in figure 2. This device shows clear resonant behaviour in both the gain and phase frequency responses as expected. The resonant frequency is around 5 MHz, the quoted resonant frequency of the commercially supplied oscillator, hence the nanocrystalline diamond deposition process has not destroyed the piezoelectric properties of the resonator. Around the resonant frequency there are small spurious an-harmonic resonances, but these were also visible before the deposition of the nanocrystalline diamond, albeit at lower relative intensities. These are due to crystalline imperfections in the langasite and surface roughness. They are generally not seen in quartz microbalances due to the lower piezoelectric coupling of quartz compared to langasite and $GaPO_4$. As they have significantly lower amplitudes and are a reasonable distance from the main resonant frequency they do not affect the operation of the device with commercial microbalance electronics.[19]

Figure 3 shows that as well as operating in air as expected, the langasite thickness shear mode resonator also operates in liquid. There is a slight downward shift in frequency due to loading at the crystal surface and a very slight damping of the oscillator due to the enhanced viscosity of the medium. Otherwise the oscillation of the crystal is not hampered by the aqueous medium and thus the device has potential for a nano-graviometric biosensor in liquid.

Thus, figures 2 and 3 show that langasite is capable of maintaining its piezoelectric properties after the CVD diamond growth process. In order to improve the device, the electrode structure was modified. In figure 1(a) the resonator is driven by the a.c. voltage setup between the gold contacts on either side of the langasite. The nanocrystalline diamond is grown on top of a SiO_2 buffer layer and thus is electrically isolated from the top contact. This electrical isolation is neither necessary nor desirable for the device operation, for example this device could not be used for simultaneous electrochemistry, as there is no electrical contact to the diamond. Thus an alternative design was used where the interlayer supporting diamond growth was switched to tungsten. Tungsten is well known to support diamond growth and is a standard refractory metal. Thus the electrode is a very thin layer of tungsten to facilitate diamond growth with around 100 nm of boron doped nanocrystalline diamond grown on top as shown in figure 1(b). This device has the considerable advantages of much lower loading due to thinner metal interlayer and no SiO_2 buffer layer, with the added bonus of electrochemical access to the diamond layer. The frequency response of this device is shown in figure 4. It can be seen from this figure that the resonant frequency is considerably lower in this device, around 2.7 MHz. Considering that the langasite substrate used in this device was 500 μm, around twice the thickness of the previous substrates, this is to be expected and confirms the thickness shear mode resonance characteristics of the langasite / nanocrystalline diamond nanobalance. An SEM of the nanocrystalline diamond layer grown on the tungsten interlayer is shown in figure 5. It can be seen that the grains size is around 50 nm with some larger crystals presumably where the seeding density was not as high.

A prototype $GaPO_4$ microbalance is shown in figure 6. Due to the chemical instability of $GaPO_4$, it was found that the tungsten interlayer and bare $GaPO_4$ were substantially etched in the microwave plasma and no significant diamond growth occurred. In order to circumvent this, the structure in Figure 1(a) was used with the langasite replaced with $GaPO_4$. In figure 6 the phase response is plotted against frequency for the $GaPO_4$ resonator both before and after diamond growth. It can be seen that in fact, the response has changed very little by exposure to the harsh diamond growth environment. Again, there are several resonating peaks, presumably due to crystalline imperfection. There is a very small downshift in all the visible peaks and some broadening after nanocrystalline diamond deposition. Thus $GaPO_4$ can also withstand the temperature of the diamond growth plasma, even if its bare surface is rather susceptible to etching by hydrogen rich plasmas.

4. CONCLUSIONS

In summary, we have demonstrated the viability of nanocrystalline diamond coated high temperature stable piezoelectrics, namely Langasite and Gallium OrthoPhosphate. These materials maintain their piezoelectric properties after exposure to the harsh environment of diamond growth, and using a suitable interlayer it is possible to coat them with thin layers of nanocrystalline diamond. These devices have much potential for bio-sensing, electrochemical / gravimetric sensing, viscolelastic monitoring etc.

ACKNOWLEDGMENTS

This work was financially supported by the Research Programme G.0068.07 of the Research Foundation - Flanders (FWO), IWT-SBO-project No. 030219 "CVD Diamond", by the IAP-P6/42 project "Quantum Effects in Clusters and Nanowires" and the EU FP6 Marie Curie RTN "DRIVE" MRTN-CT-2004-512224. MD (Research Assistant) and KH (Postdoctoral Fellow) are funded by the Research Foundation - Flanders (FWO).

REFERENCES:

[1] G Sauerbrey, Zeitschrift Fur Physik 155, 206 (1959).

[2] B. Shao, Q. Hu, J. M. Hu, X. Y. Zhou, W. M. Zhang, X. H. Wang, and X. R. Fan, Fresenius Journal of Analytical Chemistry 346 (10-11), 1022-1024 (1993).

[3] A. J. C. Eun, L. Q. Huang, F. T. Chew, S. F. Y. Li, and S. M. Wong, Phytopathology 92 (6), 654-658 (2002).

[4] M. Rodahl and B. Kasemo, Review of Scientific Instruments 67 (9), 3238-3241 (1996); B. Seantier, C. Breffa, O. Felix, and G. Decher, Nano Letters 4 (1), 5-10 (2004).

[5] K. K. Kanazawa and J. G. Gordon, Analytica Chimica Acta 175 (SEP), 99-105 (1985).

[6] C. Eickes, J. Rosenmund, S. Wasle, K. Doblhofer, K. Wang, and K. G. Weil, Electrochimica Acta 45 (22-23), 3623-3628 (2000).

[7] W. Yang, O. Auciello, J. E. Butler, Cai W., J. A. Carlisle, J. Gerbi, D. M. Gruen, T. Knickerbocker, T.L. Lasseter, J. N. Russell, L.M. Smith, and R. J. Hamers, Nature Materials 1 (4), 253-257 (2002).

[8] A. Erdemir, C. Bindal, G. R. Fenske, C. Zuiker, A. R. Krauss, and D. M. Gruen, Diamond and Related Materials 5 (9), 923-931 (1996).

[9] Christian G. Specht, Oliver A. Williams, Richard B. Jackman, and Ralf Schoepfer, Biomaterials 25 (18), 4073-4078 (2004).

[10] M. Tachiki, T. Fukuda, K. Sugata, H. Seo, H. Umezawa, and H. Kawarada, Japanese Journal of Applied Physics 39 (7B), 4631 (2000).

[11] M. Hupert, A. Muck, R. Wang, J. Stotter, Z. Cvackova, S. Haymond, Y. Show, and G. M. Swain, Diamond and Related Materials 12 (10-11), 1940-1949 (2003).

[12] W.L. Bragg and R.E. Gibbs, Proceedings of the Royal Society A 109, 405-427 (1925).

[13] Y. R. Zhang, S. Asahina, S. Yoshihara, and T. Shirakashi, Journal of the Electrochemical Society 149 (11), H179-H182 (2002).

[14] I. A. Andreev, Technical Physics 49 (9), 1101-1103 (2004).

[15] D. Damjanovic, Current Opinion in Solid State & Materials Science 3 (5), 469-473 (1998).

[16] Oliver A. Williams, Olivier Douheret, Michael Daenen, Ken Haenen, Eiji Osawa, and Makoto Takahashi, Chemical Physics Letters In Press, Accepted Manuscript, doi: 10.1016/j.cplett.2007.1007.1091 (2007).

[17] O. A. Williams, M. Daenen, J. D'Haen, K. Haenen, J. Maes, V. V. Moshchalkov, M. Nesladek, and D. M. Gruen, Diamond and Related Materials 15 (4-8), 654-658 (2006).

[18] R. Haubner, A. Lindlbauer, and B. Lux, International Journal of Refractory Metals & Hard Materials 14 (1-3), 119-125 (1996).

[19] O. A. Williams, V. Mortet, M. Daenen, and K. Haenen, Applied Physics Letters 90 (6), 063514 (2007).

FIGURE CAPTIONS:

Table 1: Comparison of the properties of ∝-Quartz, Langasite and Gallium Orthophosphate.

Figure 1: (a) Schematic of a prototype langasite oscillator with seeded SiO_2 interlayer to facilitate nanocrystalline diamond growth. (b) Schematic of second prototype langasite oscillator with seeded W interlayer to facilitate boron doped nanocrystalline diamond growth. In this device both the W interlayer and the doped nanocrystalline diamond act as the electrode.

Figure 2: Gain / Phase plots of the frequency response of the prototype langasite oscillator shown in figure 1(a).

Figure 3: Phase / frequency response of langasite oscillator in air and liquid. (the one shown in Figure 1(a))

Figure 4: Phase/ frequency response of 500μm thick langasite oscillator with tungsten interlayer.

Figure 5: Scanning Electron Micrograph of nanocrystalline diamond layer on tungsten / langasite.

Figure 6: Phase / frequency response of $GaPO_4$ resonator before and after nanocrystalline diamond growth.

	∝-Quartz	Langasite	$GaPO_4$
Density	2648 kg m^{-3}	5748 kg m^{-3}	3570 kg m^{-3}
Curie temperature	575 ºC	-	970 ºC
Melting point	1723 ºC	1475 ºC	1300 ºC
Electromechanical coupling factor (BAW)	7 %	15.8 %	19 %

Add the explanation of BAW in the caption.

Table 1

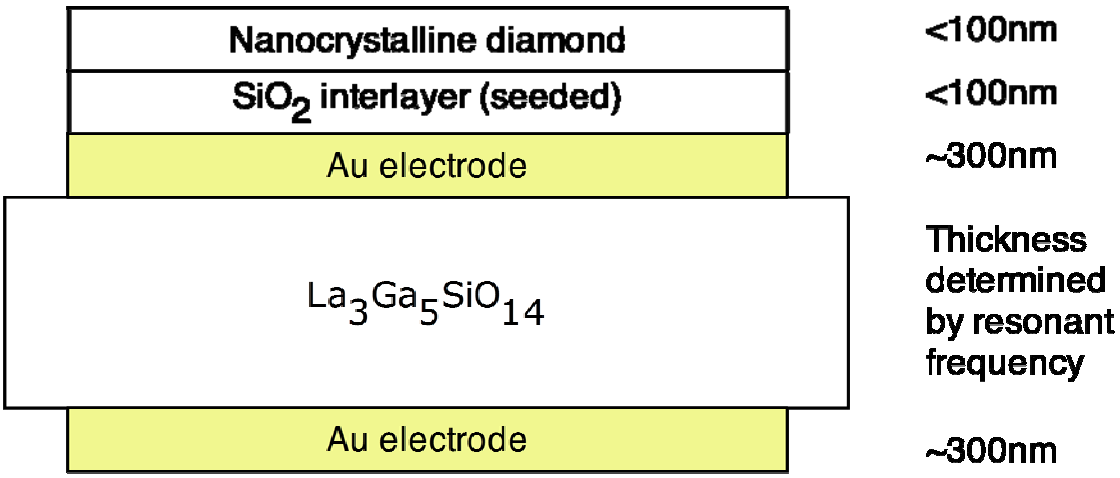
Nanocrystalline diamond
SiO_2 interlayer (seeded)
Au electrode
$La_3Ga_5SiO_{14}$
Au electrode
<100nm
<100nm
~300nm
Thickness determined by resonant frequency
~300nm

Figure 1(a)

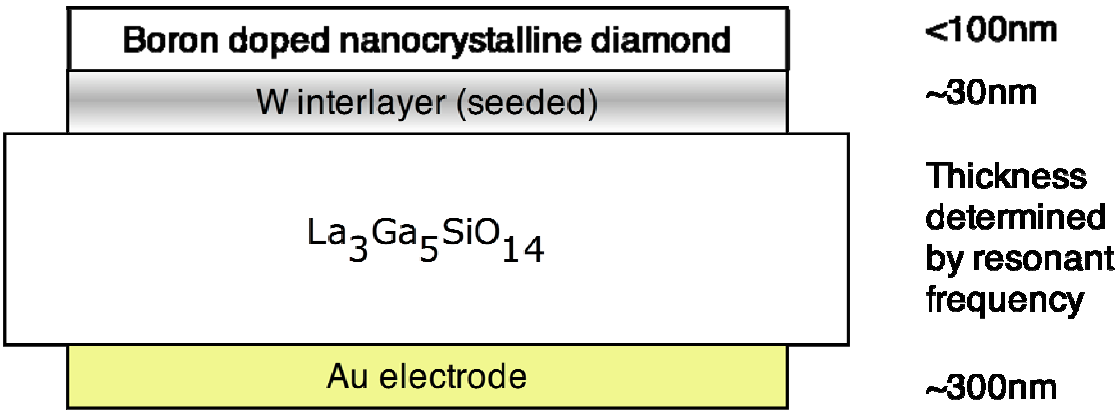
Boron doped nanocrystalline diamond
W interlayer (seeded)
$La_3Ga_5SiO_{14}$
Au electrode
<100nm
~30nm
Thickness determined by resonant frequency
~300nm

Figure 1(b)

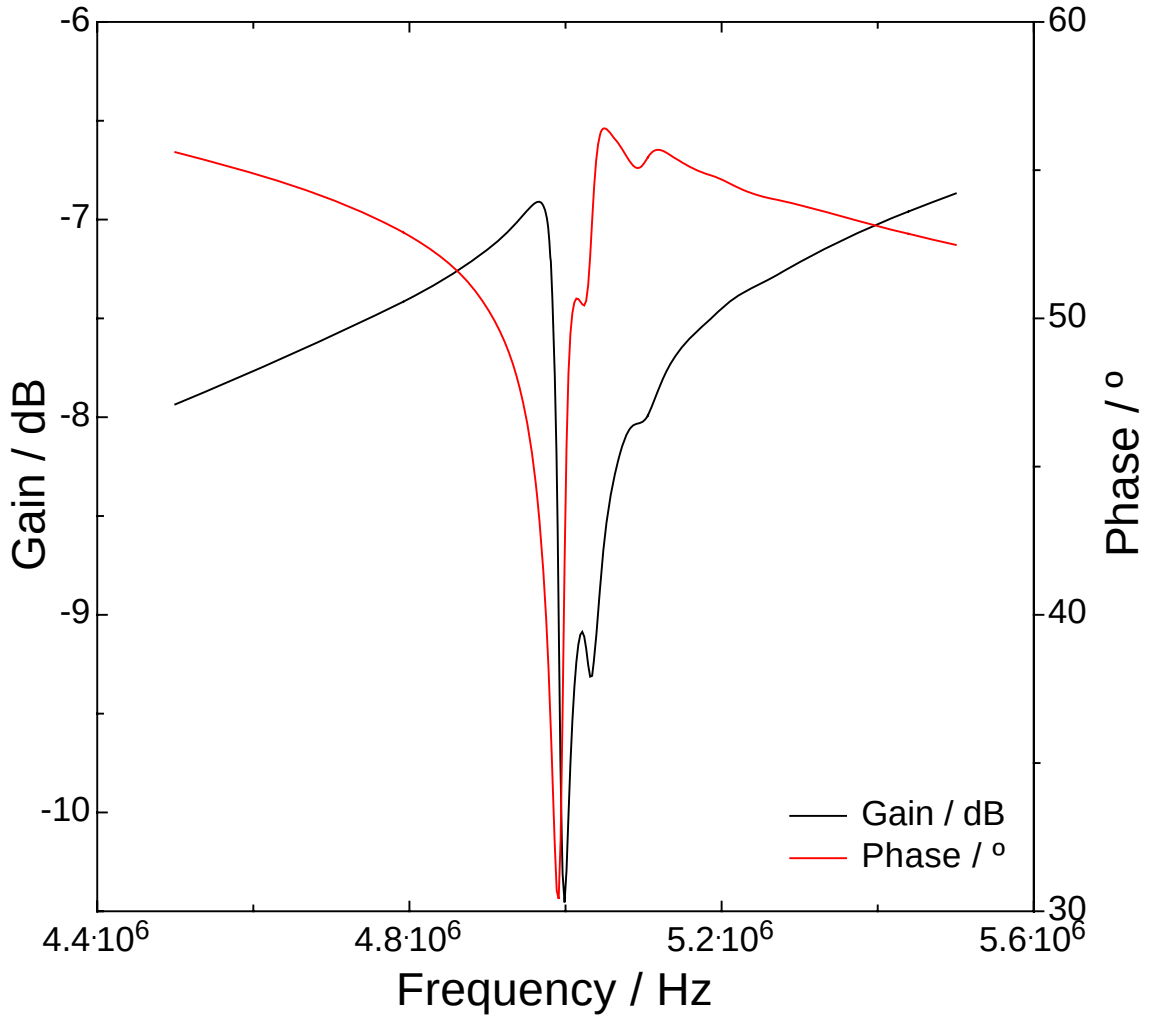

There is not much difference between the red and black curves when printed. Add arrows to denote which Y-axis corresponds with a certain curves. Add a title to the Y-axis.

Figure 2

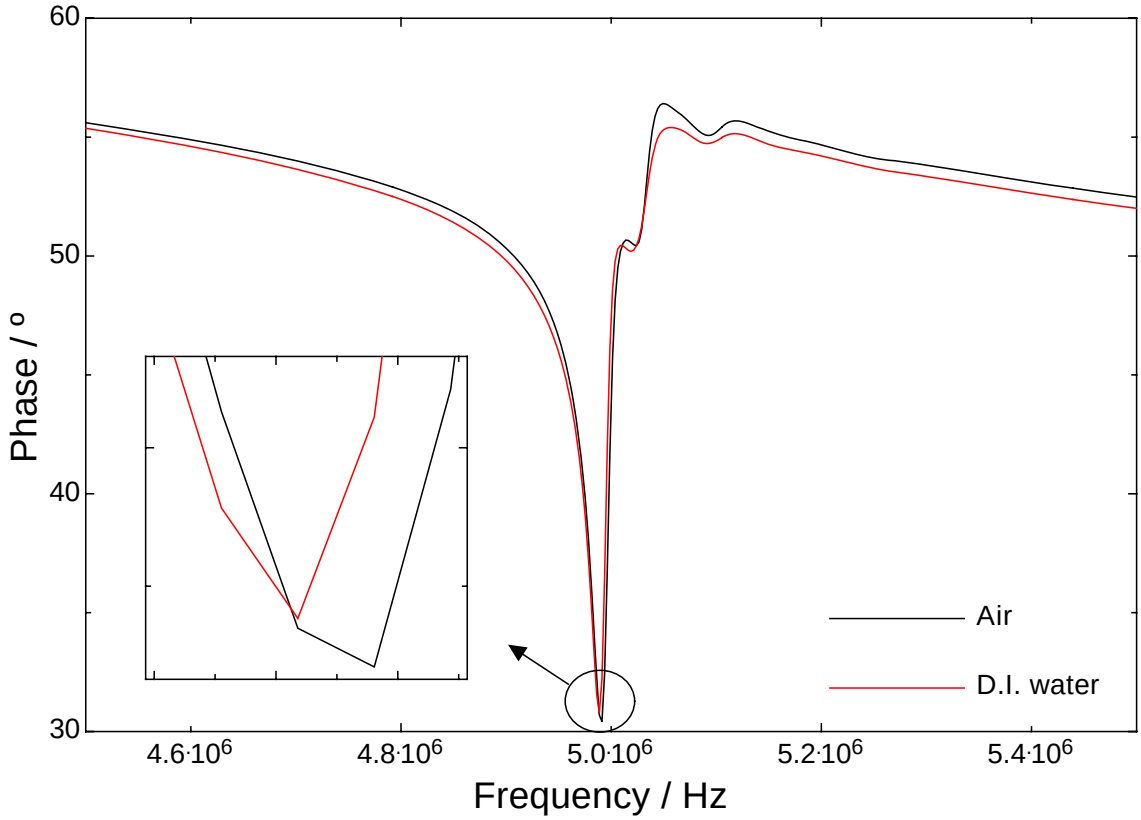

There is not much difference between the red and black curves when printed. Add a symbol or change one curve from solid to dotted line. Add a title to the Y-axis.

Figure 3

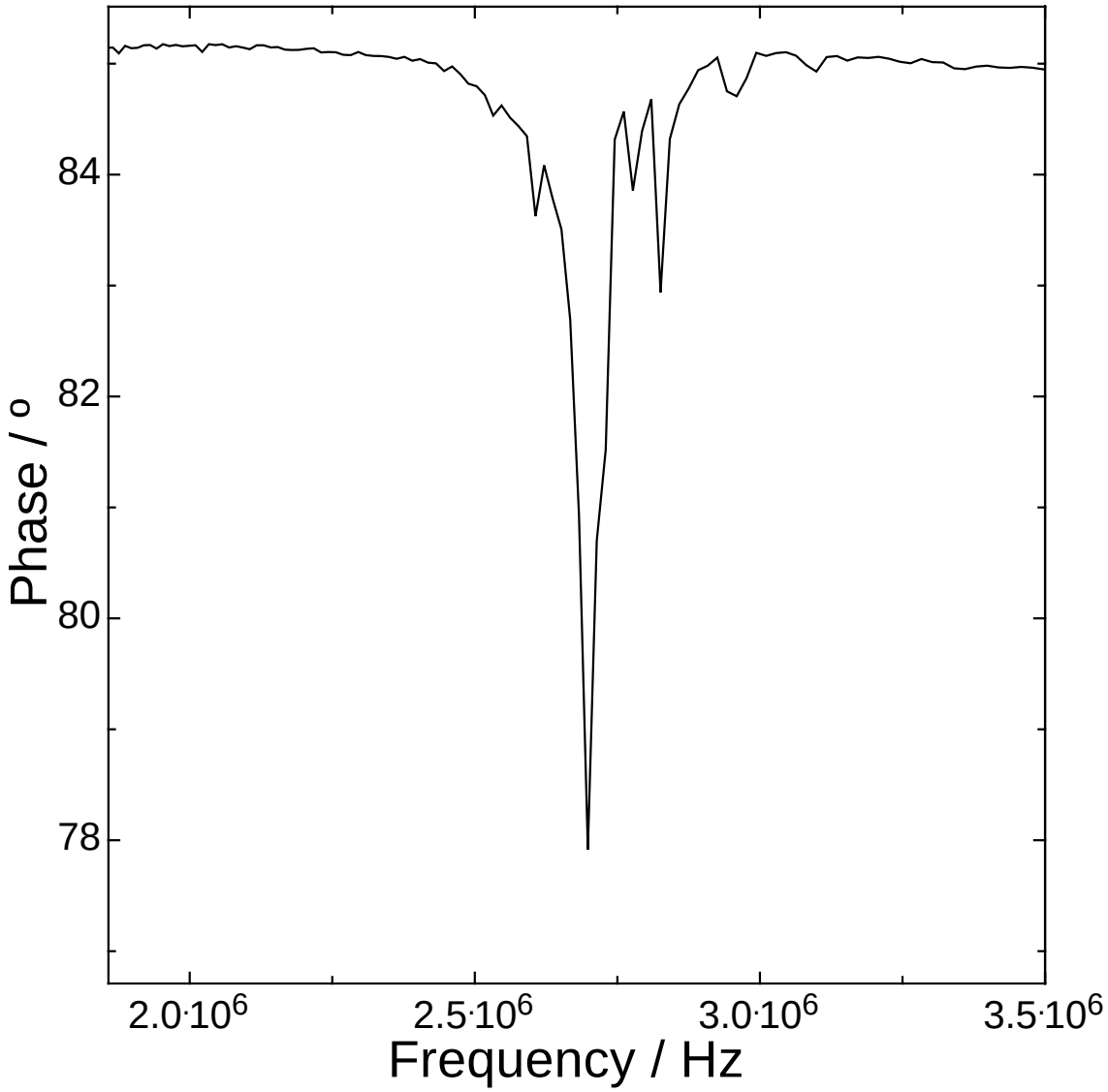

Add a title to the Y-axis.

Figure 4

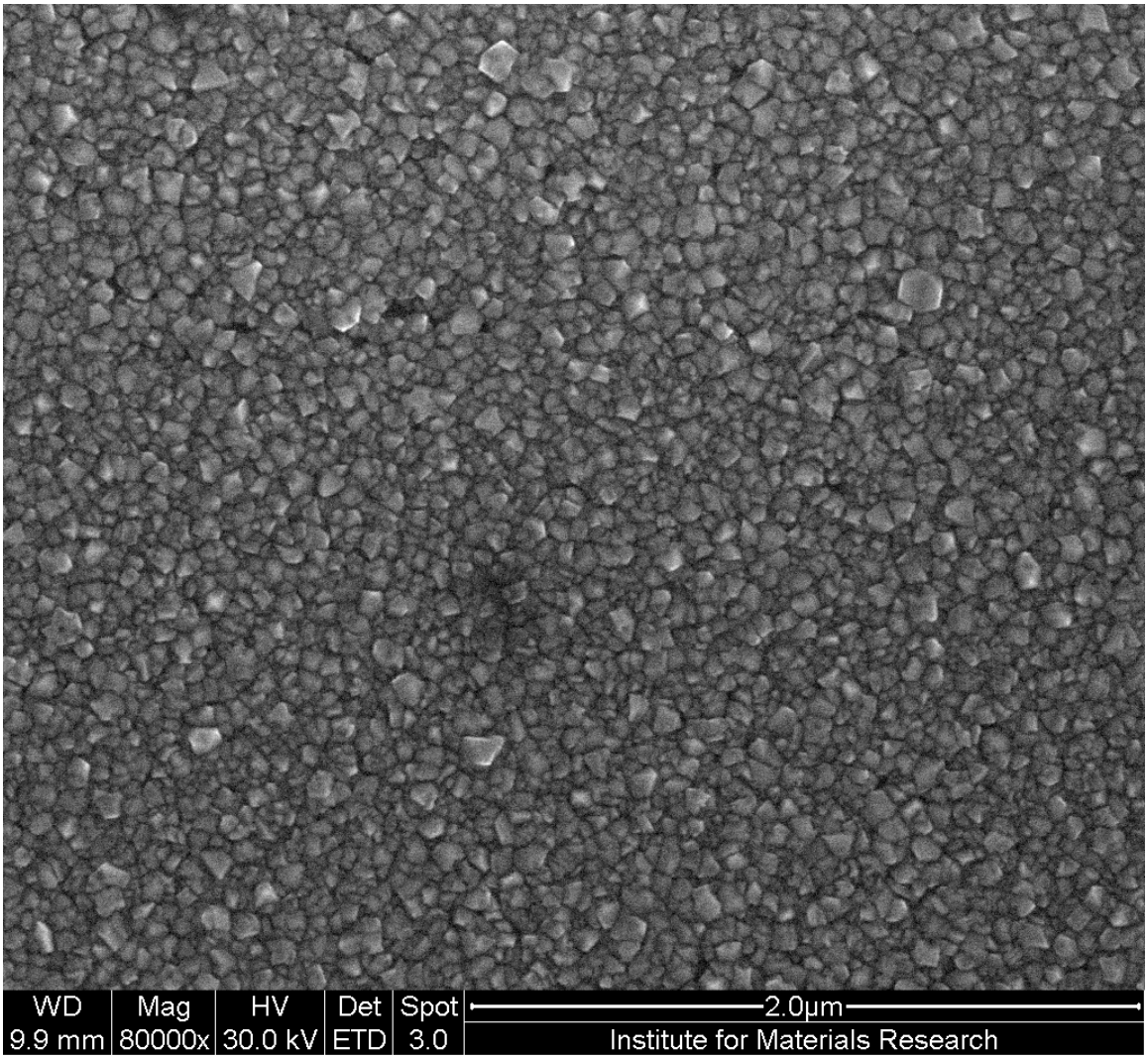
WD
9.9 mm
Mag
80000x
HV
30.0 kV
Det
ETD
Spot
3.0
2.0µm
Institute for Materials Research

Figure 5

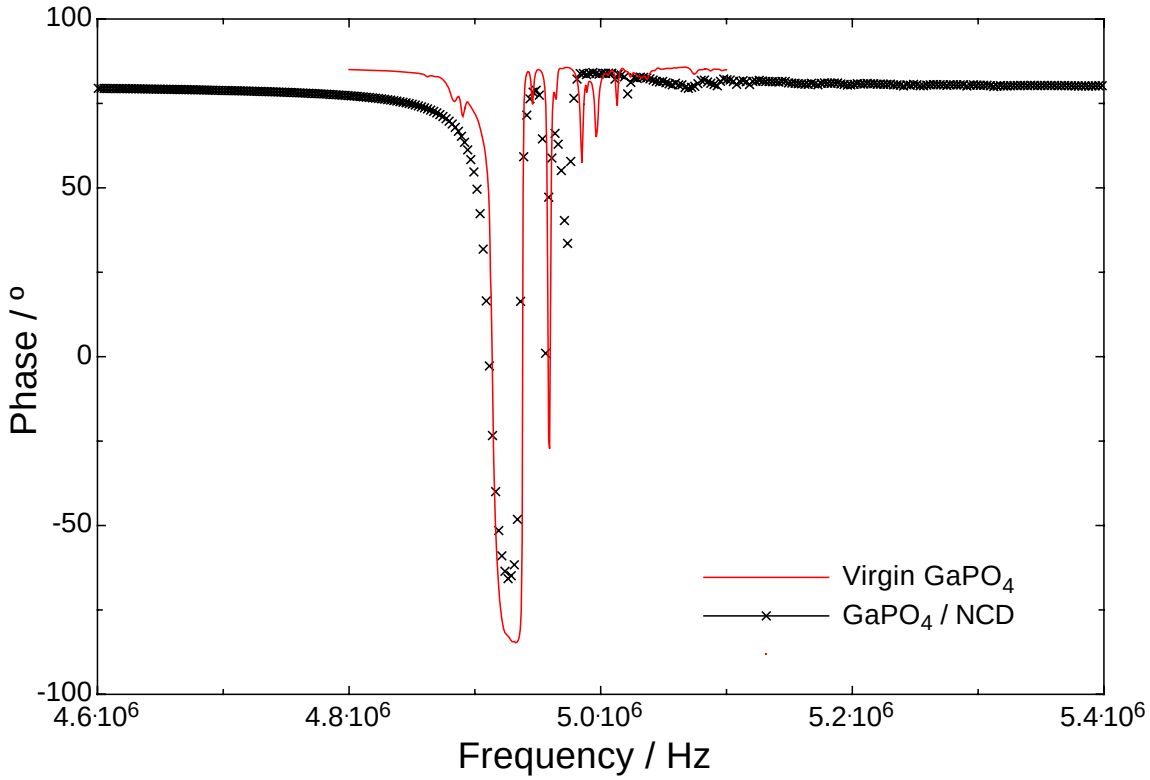

Add a title to the Y-axis.

Figure 6